Development and Investigation of Precision Laser-Interferometric Meter for Distance and Displacement Monitoring

Iu.B. Minin
Skolkovo Institute of Science and Technology,
Moscow Institute of Physics and Technology
Moscow, Russia
iurii.minin@skoltech.ru

V.M. Shevchenko
Bauman Moscow State Technical University
(National Research University of Technology)
Moscow, Russia
bmstuwangov@gmail.com

M.N. Dubrov
Fryazino Branch of Kotel'nikov Institute
of Radio-Engineering and Electronics of RAS
Fryazino, Moscow Region, Russia
mnd139@ire216.msk.su

***Abstract* — The novel method of performing high-precision monitoring of absolute distance to the reflecting object is considered. The proposed measurement principle combines electronic method of determining distances and interferometric method of recording displacements using the measurement of interference fringe fraction.**

Keywords — laser interferometer, pathfinder, helium-neon laser

I. Introduction

High precision laser metrology systems are now widely involved in modern Earth sciences and space technology. In particular, laser interferometric strainmeters are used for registration of earth surface deformations in geodesy, and geophysics [1, 2]. Precise laser interferometric pathfinders are developed for Gravity Recovery and Climate Experiment (GRACE) - mission to map the Earth's gravity field with higher resolution [3] and for free-falling test mass tracking in a space-borne gravitational wave detector [4]. For high-precision experiments, stable reference and frequency-controlled laser are required.

Known high-precision monitoring instruments and installations are based on either the radio-optical (microwave modulation) or interferometric method to determine the absolute distances. The electronic radio-optical (microwave modulation) method has the accuracy of the order of 0.1−0.2 mm. On the other hand, the interferometric method, which consists in calculating the interference fringes arising from the reflection of the light beam from the mirror, when moving the mirror from the laser to the measured point, has interference accuracy [5, 6]. However, such measuring devices are large and require the movement of mirrors. Thus, devices based on the radio-optical method do not require the movement of mirrors, but thousands of times less accurate, unlike measuring devices based on the interferometric method.

The purpose of this work is to create a device that combines the advantages of devices based on these methods: both interferometric and radio-optical. This means that the proposed device will not require the movement of mirrors and will have the accuracy of measuring the distance to the reflecting object of the order of accuracy of the interferometer.

II. Proposed method description

A. Laser modes, frequencies and their use

The proposed device combines radio-optical and interferometric methods for determining the absolute distance to the reflecting object. It is based on the physical existence of the amplitude modulation of laser radiation, which is a consequence of the presence of optical modes. The number of laser modes is determined by the parameters of the laser emitter: the length of the laser resonator, the properties of its active medium, the curvature of its mirrors, etc.

The resonant frequencies at which the generation occurs are determined from the condition of the multiplicity 2π of the phase incursion of the wave after the double pass between the resonator mirrors [7]:

$$\frac{4\pi\nu_m nL}{c} - \theta_q = 2\pi m, \qquad (1)$$

where m is the number of the longitudinal mode of the laser cavity, n is the refractive index of the active medium, L is the laser cavity length, c is velocity of light in vacuum, θ_q is the phase shift, which is determined by the presence of a transverse types of oscillation and the curvature of the resonator mirrors of the laser.

From the ratio (1) we obtain an expression for the resonance frequency:

978-1-7281-1814-7/19/31.00

$$\nu_m = \frac{c}{2Ln}\left(m - \frac{\theta_q}{2\pi}\right). \quad (2)$$

The phase shift θ_q in this case is inconsequential because of the lack of transverse types, oscillations of higher-order TEM_{0q} and TEM_{q0}. In this case, the main type of oscillations TEM_{00} is used. From the formula (2), it follows that the frequency of the radiation can be controlled by varying the length of the laser cavity. This can be done by changing its temperature. With the expansion of the resonator by increasing its temperature, the frequency of each optical mode decreases. Conversely, as the temperature of the resonator decreases, its length decreases that increases the frequency of each optical mode. This feature is used to create a laser interferometric distance and displacement meter.

For a rough measurement of the distance to the reflecting object, the number of spatial periods of the envelope of the optical modulated signal arising from the presence of several optical modes of laser radiation is calculated. In this case, the properties of the interferometer operating at several optical frequencies are used, in particular, the dependence of the interferogram visibility on the ratio of the monitored length, the length of the laser resonator, the intermodal frequency beats and the properties of the active medium. In this case, the intermodal frequency is changed by increasing the length of the resonator, for example, when it is heated.

For accurate measurements in the interferometer, the number of interference fringes is calculated, the period of which is $\lambda/2$, where λ is the wavelength of the laser used.

B. Two-mode regime

Let us consider two plane unidirectional waves with different but close frequencies corresponding to two longitudinal modes of the laser:

$$U_1 = U_{10}\sin\left(2\pi\nu_1 t - k_1 x\right) \quad (3)$$

and

$$U_2 = U_{20}\sin\left(2\pi\nu_2 t - k_2 x\right), \quad (4)$$

where U_{10} and U_{20} are the amplitudes of two waves, for example, in the reference arm of an interferometer of length L, ν_1 and ν_2 are eigenfrequencies of the resonator for two modes, $k_1 = 2\pi\nu_1 / c$ and $k_2 = 2\pi\nu_2 / c$ are wave numbers of modes, t is wave propagation time, x is wave propagation direction.

We find the appearance of the interference pattern for one mode of laser radiation with a frequency of ν_1, then, we solve the problem of adding oscillations of the same frequency, but with different phases. As a result, the intensity of the interference pattern has the form:

$$I_1 = U_{10}^2 + U_{11}^2 + 2U_{10}U_{11}\cos\left(k_1 l\right), \quad (5)$$

where U_{11} is the amplitude of the wave in the measuring arm, l is the optical path difference. The intensity at the maximum of the interference pattern $I_{1max} = (U_{10} + U_{11})^2$, and in the minimum $I_{1max} = (U_{10} - U_{11})^2$. Therefore, the visibility is

$$V_1 = \frac{I_{1max} - I_{1min}}{I_{1max} + I_{1min}} = \frac{2\sqrt{\delta_1}}{1+\delta_1}, \quad (6)$$

where the parameter

$$\delta_1 = \frac{U_{11}^2}{U_{10}^2} \quad (7)$$

expresses the ratio of the intensities of interfering waves. Visibility $V_1 = 1$ only when the interfering waves have equal intensity.

For two modes of laser radiation, the light intensity in the interference pattern is equal to the sum of the intensities of the individual modes

$$I = U_{10}^2\left[1 + \delta_1 + 2\sqrt{\delta_1}\cos\left(k_1 l\right)\right] + \\ + U_{20}^2\left[1 + \delta_2 + 2\sqrt{\delta_2}\cos\left(k_2 l\right)\right]. \quad (8)$$

The parameter δ_1, which was taken into account in (7), is determined by the light wave separation device (in a triple-mirror interferometer this is the third external reflector), and it does not depend on the mode number, i.e. $\delta_1 = \delta_2 = \delta$.

Let us find the appearance of the interference pattern for the two modes. To do this, using trigonometric transformations, and the fact that $\nu = \frac{\nu_1 + \nu_2}{2}$ is the average value of the frequencies, $\Delta\nu = \nu_2 - \nu_1$ is the intermodal frequency, we rewrite the expression (8) in the following form:

$$I = B + \sqrt{(M_1\cos(Kl))^2 + (M_2\sin(Kl))^2}\cos(kl - \phi), \quad (9)$$

with change of variables: $B = (U_{10}^2 + U_{20}^2)(1+\delta)$, $M_1 = 2\sqrt{\delta}(U_{10}^2 + U_{20}^2)$, $M_2 = 2\sqrt{\delta}(U_{10}^2 - U_{20}^2)$, $K = \frac{\pi\Delta\nu}{c}$, $k = \frac{2\pi\nu}{c}$ and $\tan(\phi) = \frac{M_2}{M_1}\tan(Kl)$

As $k >> K$ then according to (9),

$$I_{max} \approx B + \sqrt{(M_1\cos(Kl_{max}))^2 + (M_2\sin(Kl_{max}))^2}, \quad (10)$$

$$I_{min} \approx B - \sqrt{(M_1\cos(Kl_{min}))^2 + (M_2\sin(Kl_{min}))^2}, \quad (11)$$

namely, I reaches a local maximum I_{max} at $l = l_{max} \approx (\varphi(l_{max}) + 2\pi p)/k$, and a minimum I_{min} at $l = l_{min} \approx (\varphi(l_{min}) + \pi(2p+1))/k$, where p is an integer. The amplitude $\sqrt{(M_1\cos(Kl))^2 + (M_2\sin(Kl))^2}$ remains approximately constant between adjacent fringes of laser radiation intensity.

Let us consider $l_{min} \approx l_{max} \approx l$. Then, we substitute (10), (11), B, M_1, K and M_2 in the definition of visibility $V = \frac{I_{max} - I_{min}}{I_{max} + I_{min}}$ and obtain:

$$V(l) = V_1 V_2(l) \approx \frac{2\sqrt{\delta}}{1+\delta}\frac{\sqrt{U_{10}^4 + U_{20}^4 + 2U_{10}^2U_{20}^2\cos\left(\frac{2\pi\Delta\nu}{c}l\right)}}{U_{10}^2 + U_{20}^2}, \quad (12)$$

where the function

$$V_2(l) \approx \frac{\sqrt{U_{10}^4 + U_{20}^4 + 2U_{10}^2 U_{20}^2 \cos\left(\frac{2\pi\Delta\nu}{c} l\right)}}{U_{10}^2 + U_{20}^2} \qquad (13)$$

describes the dependence of the visibility from the geometric path difference l of interfering waves, the frequency difference $\Delta\nu$ and the intensity of modes U_{10}^2 and U_{20}^2. Thus, when the in-phase addition of the light waves of the two modes (i.e., according to (2), in $l = 2Lw$, where w is an integer), $V_2(l) \approx 1$ and $V(l) \approx V_1$, which coincides with the visibility of the interference pattern formed by two light waves of the same frequency, corresponding to (6).

Accuracy of the found values of the visibility: Taking into account the alteration of the amplitude $\sqrt{(M_1\cos(Kl))^2 + (M_2\sin(Kl))^2}$ in the transition from the maximum intensity at l_{max} to the minimum intensity at l_{min}, we obtain an absolute algorithmic visibility error $V(l)$ by using the method of partial derivatives [8]

$$\delta V = \left|\frac{\partial V(r_{max}, r_{min})}{\partial r_{max}}\right| \delta r_{max} + \left|\frac{\partial V(r_{max}, r_{min})}{\partial r_{min}}\right| \delta r_{min} = \frac{2B(I_{max} + I_{min} - 2B) + 2(I_{max} + I_{min} - 2B)^2}{(I_{max} + I_{min})^2}, \qquad (14)$$

where r_{max} and r_{min} are values of amplitude $\sqrt{(M_1\cos(Kl))^2 + (M_2\sin(Kl))^2}$ at l_{max} and l_{min} respectively. Then the relative algorithmic error

$$\varepsilon_V = \frac{4B^2}{I_{max}^2 - I_{min}^2} - \frac{2B}{I_{max} - I_{min}} + 2\frac{I_{max} + I_{min}}{I_{max} - I_{min}}. \qquad (15)$$

C. Doppler profile

He-Ne laser was used in the scheme of the device. The laser wavelength λ = 633 nm, the Doppler width of the gain curve $\Delta\nu_D$ = 1.5 GHz. Doppler profile may contain several optical modes in the dependence of the length of the laser cavity (2). The two-mode regime is implemented for the laser cavity length L between 10 and 20 cm.

The change in the resonator temperature leads to a different arrangement of optical modes relative to the Doppler gain curve, and, hence, leads to a change in the amplitude of each optical mode depending on the temperature of the resonator body. Longitudinal mode positions relative to the Doppler gain curve and the dependence of visibility $V_2(l)$ on the monitored distance from the laser to the reflecting object $l/2$ change due to the increase in the cavity length L. The ratio $J = U_{10}^2 / U_{20}^2$ between the intensities U_{10}^2 and U_{20}^2 of 2 optical modes ν_m and ν_{m+1} determines values V_{2min} of the visibility V_2 at local minimums (13), namely

$$V_{2min} \approx \begin{cases} 0, & \text{if } J \approx 1 \\ 1, & \text{if } J \approx 0 \text{ or } J >> 1 \end{cases} \qquad (16)$$

According to (2), the intermodal frequency is

$$\Delta\nu = \frac{c}{2Ln(\nu)}, \qquad (17)$$

where $n(\nu)$ is the refractive index depending on the frequency ν due to the dispersion characteristics of the active medium of the laser.

To find this dependence, we introduce a complex susceptibility of the medium

$$\chi = \chi' - i\chi'', \qquad (18)$$

where χ' and χ'' are respectively, real and imaginary parts of it, and i — imaginary unit.

According to [7, 9], the laser generation condition (2) can be presented in the following refined form:

$$\frac{2\pi\nu_m n}{c} L\left[1 + \frac{\chi'(\nu_m)}{2n^2}\right] - \tilde{\theta}_q = \pi m, \qquad (19)$$

where $\tilde{\theta}_q$ is a phase additive determined by the phase shifts occurring during reflection as well as the curvature of the laser resonator mirrors and the distance between the mirrors. The real part χ' of complex susceptibility is determined experimentally by measuring the intermodal frequency beats during the laser resonator length tuning.

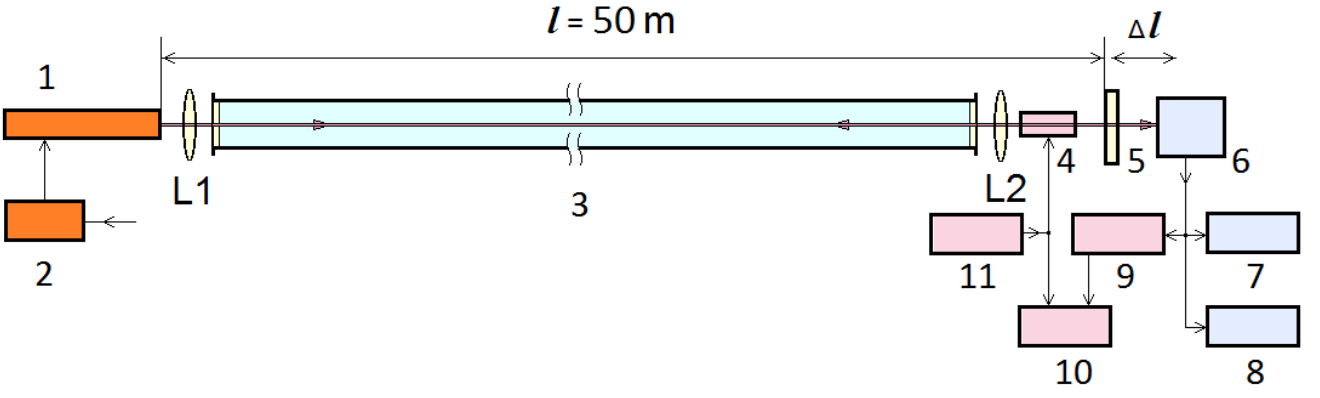

Fig. 1. Block diagram of the experimental setup

III. Experimental Study of Distance and Displacement Meter Elements

Let us consider the block diagram of the experimental setup (Fig. 1), which was used to study the dependences of the appearance of the interference pattern and the change in the intermodal frequency beats when the resonator length was changed by heating it. The laser beam is formed by the cavity mirrors of the LGN-207 model He-Ne laser 1 and by the collimating lenses L1 and L2. The laser has controlled power supply 2. The collimated laser beam enters the measuring distance *l*, which is enclosed in airtight pipe 3, then passes through the electro-optical modulator 4 and enters the partially reflecting mirror 5, fixed to the measuring rail.

The laser 1, lenses L1 and L2, enclosing airtight pipe 3 and the measuring rail with the reflecting mirror 5 are attached to the brackets, which are bricked up the wall of laboratory building. The length of the measured optical path *l* is 50 m. The airtight pipe 3 enclosing the laser beam is used to eliminate air density fluctuations over monitored distance *l*.

Part of the beam passes through the mirror 5 and focuses on the heterodyne photodetector 6. Output signal of heterodyne photodetector is supplied to the oscilloscope 7 and frequency counter 8. The part of the beam reflected from the mirror 5 returns to the laser and forms a three-mirror interferometer, the signal from which is gained by the amplifier 9 and is fed to the phasemeter 10. The oscillator 11 generates a reference signal, which controls the electro-optical modulator 4 and phasemeter 10.

Thus, on the right side of this block diagram, the dependence of the change in the intermodal frequency on the laser heating time (units 6 and 8) is studied, and the dependence of visibility on the measuring length at a changed mirror position (units 5, 6 and 7) is investigated.

Laser OKG-16 was used in the three-mirror interferometer scheme, where light beam was passed through the mirror 5, then reflected back into the laser cavity and interfered with its radiation. Then, the signal from the photodetector was analyzed on the oscilloscope 7. Thus, the visibility dependence on the change in the mirror 5 position was obtained (Fig. 2).

Here, we have used the assumption that changing the mirror 5 position varies slowly with time. Visibility varies from 0.02 to 0.15. At the point of minimum, there is a sharp change in the visibility used for the optimal setting of the frequency of a laser while changing a distance *l* (Fig. 1, Fig. 2b).

The dependence of the intermodal frequency beats on the change in the laser resonator length *L* has been investigated. The change in the intermodal frequency beats occurs in the range between 658.3 MHz and 659.2 MHz, has a periodic character with a period of λ/2, where λ = 633 nm. The observed nature of the frequency change is related to the shape of the Doppler profile [10] and is used to control the distance between the frequencies of the generated modes.

IV. Development of Interferometric Meter Scheme

The proposed device (Fig. 3) consists of four units: Laser unit with cavity mirrors M1, M2, Mirror 3 unit, Heterodyne photodetector unit and Analysis unit. Mirrors M1, M2 of the laser form a beam that enters the Mirror 3, fixed to the movable measured object, and is reflected back. At the output of the photodetector, an interference signal (DC channel) and a signal of intermode beats are generated, which are fed from the output of the heterodyne photodetector unit to the Analysis unit (AC channel). Microcontroller processes incoming signals and controls the operation of the device.

If the specified accuracy of distance and displacement measurements is λ/2, where λ – is the wavelength of its radiation, then measurements of the intermodal frequency beats with the following accuracy is required

$$\delta(\Delta\nu) = -\frac{c}{2L^2 n}\delta l \approx -\frac{c}{2L^2 n}\lambda. \tag{20}$$

If the offset of the interferogram is set with greater sensitivity, the measurement accuracy is increased.

Thus, the considered technique combines the radio-engineering method for determining distances and interferometric method for registering displacements. With the use of a fractional interference fringe meter, the distance monitoring accuracy can be greatly improved.

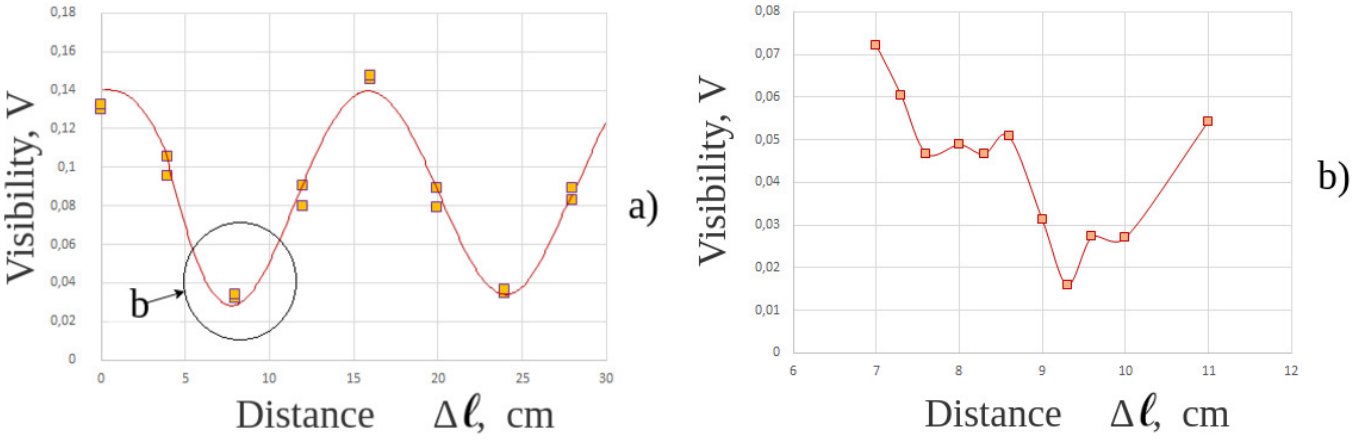

Fig. 2. Experimental visibilities versus changing in the measuring length graphs.

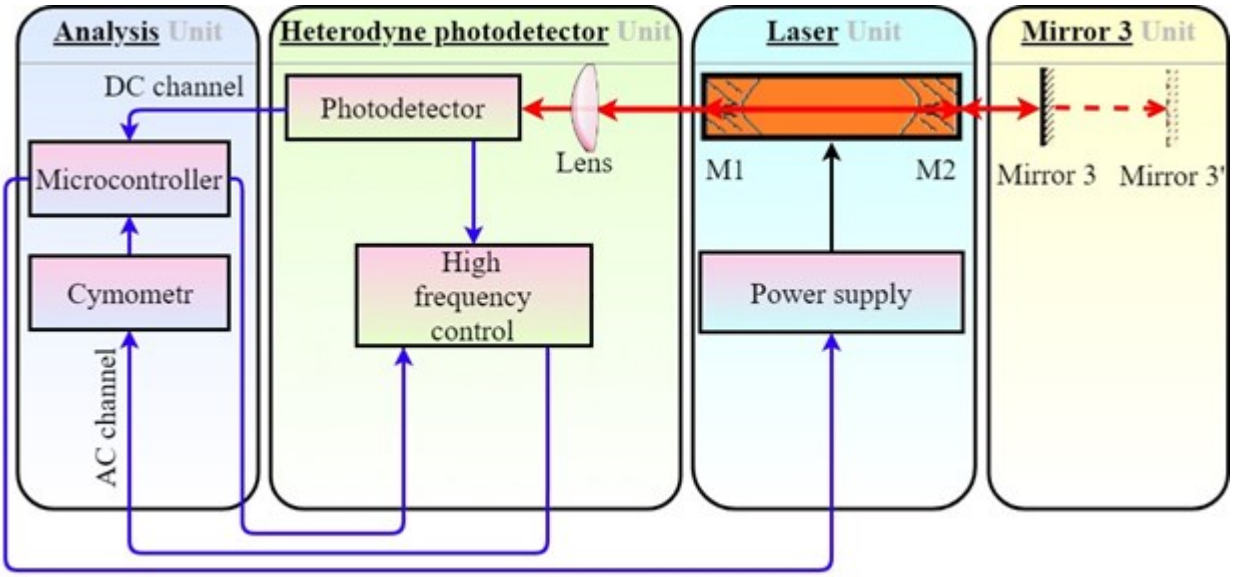

Fig. 3. Block diagram of the proposed laser interferometric distance and displacement meter

Let us consider the scope of the proposed device. These results can be applied in such areas as laser technology, devices for accurate measuring geometric quantities, environmental management, technology of prevention and damage elimination of natural disasters and man-made emergencies, transport and space system (technologies to create precise high-speed vehicles and intelligent control systems for new remote sensing and fundamental research means), nanodevices and microsystem technologies.

For high accuracy ensuring of this instrument, beam path protection is needed. The vacuum or airtight volumes (pipes, chambers) should be used for on-ground installations [1, 2]. Another way is application of high precision metrology system in free space [3, 4].

According to this scheme, a device can be developed for use on the space station for detecting gravitational waves ELISA [4, 11], which will be built in 2034.

V. Conclusion

The novel scheme of the device for monitoring of distances and object movements was created. The possibilities of using the resonator length change for the design to measure absolute distances and displacements and their application in precise interference measurements was confirmed. The proposed method is based on two-modes regime of laser operation as well as radio-optical (modulation) and interferometric techniques using. The monitoring device has possibility to improve its accuracy of measurements.

Acknowledgments

The work was carried out within the framework of the state task 0030-2019-0014.

References

[1] M. Zadro, C. Braitenberg, “Measurements and Interpretations of Tilt-Strain Gauges in Seismically Active Areas,” Earth-Sciences Reviews, vol. 47, no. 3-4, pp. 151-187, 1999.

[2] V.V. Kravtsov, M.N. Dubrov, and M.S. Remontov M.S. “Detection of solid Earth excitations by laser seismo-acoustic antenna array,” Proceedings of the 8th International conference ICATT’11, 20-23 September, 2011, Kyiv, Ukraine, pp. 117-119, IEEE Xplore Digital Library, DOI: 10.1109/ICATT.2011.6170723.

[3] Hechenblaikner G., Wand V., Kersten M., Danzmann K., Garcia A., Heinzel G., Nofrarias M., and Steier F. Digital laser frequency control and phase-stabilization loops in a high precision space-borne metrology system // IEEE Journal of Quantum Electronics. May 2011. vol. 47. pp. 651–660.

[4] D. Bortoluzzi, M.D. Lio, R Oboe, and S. Vitale, ”Spacecraft high precision optimized control for free-falling test mass tracking in LISA pathfinder mission,” in The 8th IEEE International Workshop on Advanced Motion Control, AMC ’04., pp. 553-558, March 2004.

[5] R. Bommareddi, ”Applications of Optical Interferometer Techniques for Precision Measurements of Changes in Temperature, Growth and Refractive Index of Materials,” Technologies, 2 (2), pp. 54-75, 2014.

[6] J.F. O’Brien and G.W. Neat, Micro-precision interferometer pointing control system, in Proceedings of the 4th IEEE Conference on Control Applications, pp. 464-469, Sept 1995.

[7] A. Yariv, ”Quantum electronics,” John Wiley & Sons, New York, London, Sydney, Toronto, 1975.

[8] L.A. Goodman, ”On the exact variance of products,” Journal of the American Statistical Association, vol. 55, no. 292, pp. 708-713, 1960.

[9] M.N. Dubrov, ”Long-base laser interferometry: accounting for backscattering, ” Teaching aid, MIPT, Moscow, 2011, pp. 3–9.

[10] M.O. Scully and W.E. Lamb, ”Quantum theory of an optical maser. I. General theory,” Phys. Rev., vol. 159, pp. 208-226, Jul 1967.

[11] J.J.E. Delgado, A.F.G. Marin, I. Bykov, G. Heinzel, and K. Danzmann, ”Free-space laser ranging and data communication,” in 2009 6th Workshop on Positioning, Navigation and Communication, Hannover, Germany, March 19, 2009, pp. 275-281.